Nanofiltration Modeling Based on the Extended Nernst-Planck Equation under Different Physical Modes

J.M. Gozálvez-Zafrilla* and A. Santafé-Moros
Universidad Politécnica de Valencia. Department of Chemical and Nuclear Engineering
*Corresponding author: C/ Camino de Vera s/n. 46022. Valencia (Spain), jmgz@iqn.upv.es

Abstract: Physical-based nanofiltration models describe the interaction between the membrane and multi-ionic feed solutions. Generally speaking, membrane models yield permeate composition for specified feed concentration and operating conditions. The most successful nanofiltration models are those based in the combination of the Extended Nernst-Planck equation with the Donnan steric equilibrium. As permeate composition influences the transport across the membrane, the resulting equation system is implicit. Therefore, these models have been typically solved by using iterative procedures based on the Runge-Kutta method. Nevertheless, such procedures present convergence problem in some cases. In this paper, we present an implementation of the original Donnan Steric-partitioning Pore Model (DSPM) using COMSOL. Three different physical models were used and compared (PDE coefficient form, Convection and Diffusion, Nernst-Planck without electroneutrality). The use of COMSOL benefits from the possibility of using stabilization techniques and the representation and analysis capabilities.

Keywords: Membrane, Nanofiltration, Nernst-Planck equation, DSPM.

1. Introduction

A membrane is a permselective barrier able to selectively separate components from a solution when a driving force is applied.

Nanofiltration (NF) is a pressure-driven membrane process with intermediate characteristics between ultrafiltration and reverse Osmosis. Nanofiltration membranes have pores with a diameter of the order of 1 nm and are able to effectively separate small molecules and polyvalent ions [1]. When dealing with ionic solutions, the existence of fixed charges in the membrane influences ion distribution inside the membrane (Figure 1).

NF models are intended to obtain permeate composition as a function of feed composition and operating conditions. One of the most successful models is the Donnan Steric-partitioning Pore Model (DSPM) [2], which is the basis of the most recent NF models. This model is suitable to describe the interaction between the membrane and multi-ionic solutions. The DSPM model uses the Extended Nernst-Planck equation (ENP) to describe ion transport inside the pores under the effect of drag forces. In a 1D approach, radial effects are averaged and only concentration gradients along the membrane thickness are considered. At the membrane boundaries (feed and permeate side), ion partitioning between membrane and solution is defined by the steric-Donnan equilibrium. The concentration gradient is derived from the combination of the ENP equation with the electroneutrality condition. As the concentration gradient depends on permeate concentration, the solution is obtained through an iterative procedure integrating the concentration gradient using finite differences or a Runge-Kutta method. The main drawback of this procedure is the possibility of convergence problems [3].

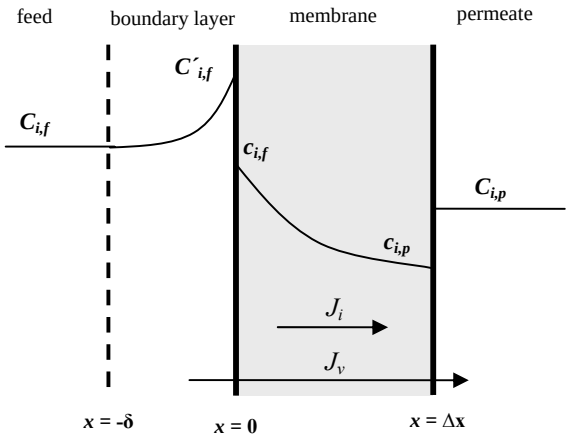

Figure 1. Solute concentration profiles in the membrane and the feed boundary layer.

2. Governing Equations

Any membrane model aims to obtain solute concentrations in the permeate $C_{i,p}$ from known solute concentrations at the feed wall $C'_{i,f}$. These concentrations will be related through the solute concentrations in the membrane c_i that are the state variables of the problem.

The DSPM considers that the solute and solvent transport takes place in cylindrical pores of known effective radius r_p and effective length Δx. The membrane has an effective membrane charge X_d.

The pressure difference established between both membrane sides causes a solvent flow inside the pore of velocity V defined by the Hagen-Poiseuille equation (eq. 1).

Solutes are drawn by convection, diffusion and electrical forces resulting in a solute flux, J_i, through the membrane. The solute transport is explained by the ENP (eq. 2) that differs from the Nernst-Planck equation on the use of drag coefficients for convection $K_{i,c}$, and diffusion $K_{i,d}$. Such coefficients are necessary to correct the convective and diffusive transport in the bulk solution for a solute confined in a pore. Expressions for the calculation of the drag coefficients can be found elsewhere [4, 5]. They exclusively depend on the ratio of the Stokes solute radius to the membrane pore radius λ_i (eq. 3). The transport equation is subjected to a set of constraints and boundary conditions. The electroneutrality conditions (eq. 6 to 8) must be fulfilled in the feed solution, membrane and permeate respectively. Besides, the compositions in the membrane at the feed wall are related to the solute compositions at the membrane through the Donnan steric-partitioning condition (eq. 9); and the same for the compositions in the membrane and permeate solution (eq. 10). The steric-partitioning coefficient Φ_i used in these equations is calculated from the aforementioned ratio λ_i. These conditions must be fulfilled separately for each solute, but depend on the Donnan potential established at each membrane side.

$$V = \frac{\Delta P\, r_p^{\,2}}{8\,\mu\,\Delta x} \tag{1}$$

$$J_i = -K_{i,d}\, D_{i,\infty}\, \frac{dc_i}{dx} + K_{i,c}\, c_i\, V + - z_i\, c_i\, K_{i,d}\, D_{i,\infty}\, \frac{F}{R_G\, T}\, \frac{d\Psi_m}{dx} \tag{2}$$

$$\lambda_i = \frac{r_i}{r_p} \tag{3}$$

$$K_{i,d} = K_d(\lambda_i, 0) \tag{4}$$

$$K_{i,c} = K_c(\lambda_i, 0) \tag{5}$$

$$\sum_i z_i\, C'_{i,f} = 0 \tag{6}$$

$$\sum_i z_i\, c_i + X_d = 0 \tag{7}$$

$$\sum_i z_i\, C_{i,p} = 0 \tag{8}$$

$$\frac{\gamma_{i,0}\, c_{i,0}}{\gamma_i C'_{i,f}} = \Phi_i\, \exp\left(-\frac{z_i\, F}{R_G\, T} \Delta\Psi_D\big|_{x=0} \right) \tag{9}$$

$$\frac{\gamma_{i,\Delta x}\, c_{i,\Delta x}}{\gamma_{i,p} C_{i,p}} = \Phi_i\, \exp\left(-\frac{z_i\, F}{R_G\, T} \Delta\Psi_D\big|_{x=\Delta x} \right) \tag{10}$$

$$\Phi_i = \begin{cases} 1-\lambda_i^{\,2} & \text{si } \lambda_i < 1 \\ 0 & \text{si } \lambda_i \geq 1 \end{cases} \tag{11}$$

3. Numerical Model

In order to implement the concentration derivatives, one must take into account that the flux of component is related to its concentration through eq. 12:

$$J_i = V\, C_{i,p} \tag{12}$$

Afterwards, by combining the ENP equation (eq. 2) with the permeate electroneutrality condition (eq. 8) the electrical gradient is obtained (eq. 13):

$$\frac{d\Psi_m}{dx} = \frac{V \sum_{j=1}^{n} z_j\, \dfrac{K_{j,c}\, c_j - C_{j,p}}{K_{j,d}\, D_j}}{\dfrac{F}{R_G\, T} \sum_{j=1}^{n} z_j^{\,2}\, c_j} \tag{13}$$

Then, from eq. 2, the gradient concentration for each component i can be expressed as a function of the state variables:

$$\frac{dc_i}{dx} = V \left\{ \frac{K_{i,c}\, c_i - C_{i,p}}{K_{i,d}\, D_i} - z_i\, c_i \frac{\sum_{j=1}^{n} z_j \frac{K_{j,c}\, c_j - C_{j,p}}{K_{j,d}\, D_j}}{\sum_{j=1}^{n} z_j^{\,2}\, c_j} \right\} \quad (14)$$

The set of equations 14 defines the membrane subdomain.

Equations 9 and 10 define the boundary conditions at both membrane sides. In our case, ideal conditions will be assumed, so the activity coefficients are set to 1. For the case of a salt solution of two electrolytes of the same charge modulus ($z_1 = -z_2$), these equations reduce to eq. 15 and 16 that express membrane concentrations as a function of the concentrations in the solution.

$$c_{1,0} = \frac{1}{2 z_1} \left(- X_d + \sqrt{X_d^2 + 4 z_1^2\, C_1' \Phi_1\, C_2' \Phi_2} \right) \quad (15)$$

$$c_{2,0} = c_{1,0} + \frac{X_d}{z_1} \quad (16)$$

Similarly, the application of the boundary condition to the permeate side yields to the permeate concentrations from membrane concentration.

$$C_{1,p} = \sqrt{\frac{c_{1,\Delta x}\, c_{2,\Delta x}}{\Phi_1\, \Phi_2}} \quad (17)$$

$$C_{2,p} = C_{1,p} \quad (18)$$

4. Modeling with COMSOL

As an example of the solution procedure, COMSOL Multiphysics was applied to solve the transport of the magnesium sulfate salt through a nanofiltration membrane.

Three different physical modes were compared and the subdomain was specified for each state variable according to each mode as later explained.

4.1 Constant definition

In the appendix, Table 1 shows the problem definition; that is, the ion concentrations in the feed, solvent velocity and temperature. Solvent velocity is consequence of the application of a certain pressure (equation 1).

Table 2 shows the membrane parameters of the DSPM used in the calculation example. The effective pore radius of the membrane is usually obtained through experiments with non-charged solutes. The parameter $\Delta x/A_k$ can be obtained using equation 1 through permeation experiments with pure solvent. The effective membrane charge X_d can be fitted by minimization of a cost function based in the model solution using data from experiments at different solute concentration.

Table 3 shows the relevant ion properties used to calculate the ion coefficients of Table 4 used in the subdomain equations. Indices are i = 1 for magnesium and i = 2 for sulfate.

Table 5 and 6 shows the universal constants used and the dependent variables of the model.

4.2 Geometry and meshing

The membrane was defined as a one-dimensional domain from 0 to $\Delta x = 1.0 \times 10^{-6}$ m (It was assumed a value of the surface porosity $A_k = 1$).

The membrane domain was meshed using 32 nodes. A greater number of nodes did not substantially improve the quality of the obtained solution.

4.3 Subdomain definition for the PDE coefficient form mode

The general stationary equation of a PDE in coefficient form is:

$$\nabla\left(-c\nabla\mathbf{c} - \alpha\,\mathbf{c} + \gamma\right) + a\,\mathbf{c} + \beta\nabla\mathbf{c} = f \quad (19)$$

Considering the concentration gradient defined by equation 14, the following terms were identified in equation 19:

$$e_a = d_a = c = \alpha = \gamma = \begin{bmatrix} 0 & 0 \\ 0 & 0 \end{bmatrix}$$

$$\beta = \begin{bmatrix} 1 & 0 \\ 0 & 1 \end{bmatrix}$$

$$a = \begin{bmatrix} -V \cdot K_{1,c} / \left(K_{1,d}\, D_1\right) & 0 \\ 0 & -V \cdot K_{2,c} / \left(K_{2,d}\, D_2\right) \end{bmatrix}$$

$$f = V \cdot \begin{bmatrix} \dfrac{-C_{1,p}}{K_{1,d}\ D_1} - c_1 \dfrac{\dfrac{K_{1,c}\ c_1 - C_{1,p}}{K_{1,d}\ D_1} - \dfrac{K_{2,c}\ c_2 - C_{2,p}}{K_{2,d}\ D_2}}{c_1 + c_2} \\ \dfrac{-C_{2,p}}{K_{2,d}\ D_2} - c_2 \dfrac{\dfrac{K_{1,c}\ c_1 - C_{1,p}}{K_{1,d}\ D_1} - \dfrac{K_{2,c}\ c_2 - C_{2,p}}{K_{2,d}\ D_2}}{c_1 + c_2} \end{bmatrix}$$

4.4 Subdomain definition for the Convection and Diffusion mode

This mode allowed us to take advantage of stabilization techniques included.

$$\nabla(-D1\nabla c1) = R1 - u \cdot \nabla c1 \qquad (20)$$
$$\nabla(-D2\nabla c2) = R2 - u \cdot \nabla c2$$

The terms R1 and R2 were set as the right hand side of eq. 14 particularized for each ion. Coefficients D1 and D2 were set to 0.

The x-velocity was set to u = 1 for both subdomain equations.

Concentration values in the domain were initialized to those calculated at the left boundary using equation 9.

4.5 Subdomain definition for the Nernst-Planck without electroneutrality mode.

Both ion concentrations do not fulfill the electroneutrality condition independently from the membrane charge. Therefore, the Nernst-Planck equation without electroneutrality had to be used.

For each ion *i*, we have:

$$\nabla \cdot \left(-D_i \nabla c_i - z_i u_{m,i} F c_i \nabla V\right) = R_i - \mathbf{u} \nabla c_i \qquad (21)$$

By comparison of eq. 21 with the ENP (eq. 2), D was taken as a corrected diffusivity (eq. 22) and the ion mobility was calculated using eq. 23. Other data required were the charge number (z_i) and the x-velocity (V).

$$D_i = D_{i,p} = K_{i,d}\ D_{i,\infty} \qquad (22)$$

$$u_{m,i} = \frac{D_{i,p}}{R_G T} \qquad (23)$$

Nevertheless, the Nernst-Planck equation does not match exactly the ENP as the latter considers a corrected convective term. Therefore, the term R_i was used to add the correction for the convective term as:

Jv*(1-Kc1)*grad_c1_chekf
Jv*(1-Kc2)*grad_c2_chekf

4.6 Boundary condition and extrusion of variables

For all cases, the left boundary condition was established as a concentration boundary condition. The solute concentrations in the membrane were calculated from the feed concentrations using equations 15 and 16.

For the "PDE coefficient form" and "Convection and Diffusion" modes the right boundary conditions was set as a free concentration boundary condition; that is, the state variables c1 and c2 were imposed. Then, c1 and c2 were used to calculate the permeate concentrations Cp1 and Cp2 using equations (17) and (18). These were used as extrusion coupling variables from the right boundary to the complete subdomain to be used in the differential equation.

For the Nernst-Planck equation without electroneutrality, this strategy could not be used. However, imposing the concentrations obtained for the other procedures conducted to similar concentration profiles.

4.6 Solver selection

The direct solver UMFPACK showed to be very efficient in terms of stability and computational speed.

At high effective membrane charge ($|X_d|$> 50), convergence difficulties occur. So, a parametric continuation technique was used. This consisted in gradually incrementing X_d from a converged solution. Using this technique with a parametric segregated solver, a solution could be achieved without difficulty in most cases.

5. Results and discussion

Either using the "PDE Coefficient form" or the "Convection and Diffusion" mode, the solution obtained agreed with the solution obtained by the classical iterative procedure based in the Runge-Kutta method [3]. Computation time using the FEM approach was slightly higher, but there were less convergence problems using the new procedure.

Comparing the "PDE Coefficient form" and the "Convection and Diffusion" modes, the latter approach showed less convergence problems. The "Convection and Diffussion" mode also had the possibility to use stabilization methods.

In the following lines, same results are shown to demonstrate the prediction capabilities of the model implemented.

Figure 2 shows the ion concentration profiles obtained at three different membrane charges for the nanofiltration of the magnesium sulfate solution of 50 mol·m^{-3}. As can be seen, a positive membrane charge causes in the one hand a higher concentration of the anion inside the membrane, being in this case slightly smaller than in the feed because of the steric effect. On the other hand the positive charge causes a drastic decrease of the cation concentration in the membrane. Inversely, for the case of a negative charge, the anion concentration is lower and the cation concentration is higher.

All the effects mentioned have a decisive effect on the transport through the membrane. For the membrane charges considered (X_d = -50, 0, +50 mol·m^{-3}) the following permeate concentration could be calculated from the ion concentrations on the left boundary: 19.0, 11.5, 3.7 mol·m^{-3}.

Figure 3 shows a parametric study of the effect of the membrane charge on the rejection index calculated using equation 24. A minimum of retention is observed for a negative near to -40 mol·m^{-3}. This kind of results can be useful to design suitable membrane for treating specific solutions.

$$R(\%) = \left(1 - \frac{C_{i,f}}{C_{i,p}}\right) \times 100 \qquad (24)$$

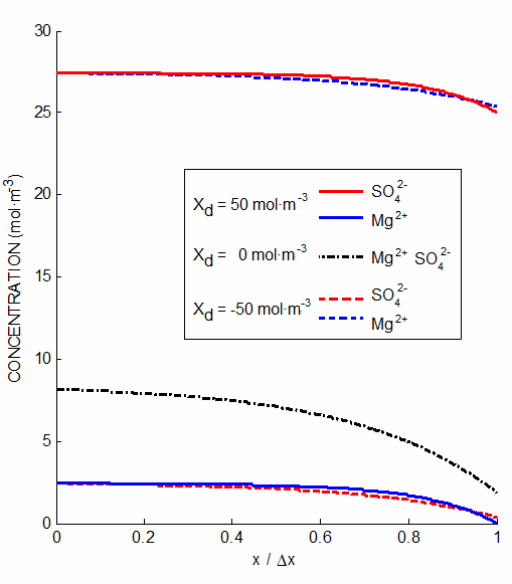

Figure 2. Ion concentrations along the membrane thickness for three different effective membrane charges.

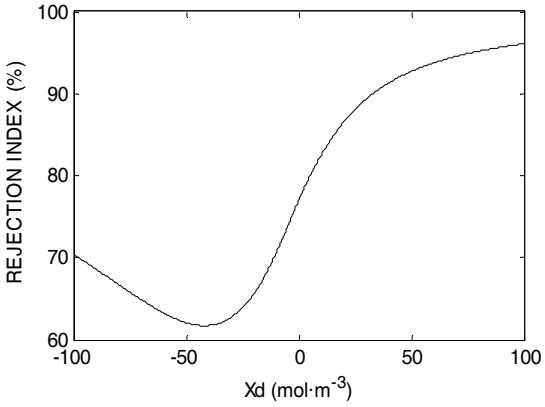

Figure 3. Effect of the membrane charge on magnesium sulphate rejection.

7. Conclusions

The use of COMSOL can greatly simplify the study and development of NF models. In many aspects, especially convergence, higher performance was obtained compared with traditional methods. Other important advantages

were a smaller time of implementation and the post-processing tools available.

The procedure can be extended to system of more ions including concentrations as additional states. The results obtained with NF models are useful for membrane design and operation.

8. References

1. Schaeffer et al., *Nanofiltration. Principles and applications*, (2005)
2. W.R. Bowen, H. Mukhtar, Characterisation and prediction of separation performance of nanofiltration membranes, *J. Membr. Sci.*, **112**, 263-274 (1996)
3. A. Santafé-Moros, J.M. Gozálvez-Zafrilla, Applicability of the DSPM with dielectric exclusion to a high rejection nanofiltration membrane in the separation of nitrate solutions, *Desalination*, **221**, 268-276 (2008)
4. C. Labbez et al., Evaluation of the "DSPM" model on a titania membrane: measurements of charged and uncharged solute retention, electrokinetic charge, pore size, and water permeability, *Journal of Membrane Science*, **208**, 315-329 (2002)
5. W.R. Bowen et al., Characterisation of nanofiltration membranes for predictive purposes - Use of salts, uncharged solutes and atomic force microscopy, *Journal of Membrane Science*, **126**, 91-105 (1997)

9. Acknowledgements

Authors wish to thank to the project GV/2007/197 of the Conselleria d'Educació de la Generalitat Valenciana for the financial support to this study.

10. Appendix

Table 1: Problem specification

Param.	Value	Description
$C'_{1,f}$	50	Feed magnesium concentration ($mol \cdot m^{-3}$)
$C'_{2,f}$	50	Feed sulfate concentration ($mol \cdot m^{-3}$)
V	10^{-4}	Solvent velocity ($m \cdot s^{-1}$)
T	298	Temperature (K)

Table 2: DSPM membrane parameters

Param.	Value	Description
r_p	0.5	Effective pore radius (nm)
$\Delta x/A_k$	1.0	Ratio of the effective pore length to the surface pore area (μm)
X_d	[-30, 30]	Effective membrane charge ($mol \cdot m^{-3}$)

Table 3: Ion properties

Param.	Mg^{+2} (i=1)	SO_4^{-2} (i=2)	Description
z_i	1.350	1.467	Ion charge
$D_{i,\infty}$	0.70×10^{-9}	1.06×10^{-9}	Bulk diffusivity ($m^2 \cdot s^{-1}$)
$r_{S\,i}$	0.348	0.231	Solute radius (nm)

Table 4: Calculated ion parameters for r_p = 0.5 nm

Param.	Mg^{+2} (i=1)	SO_4^{-2} (i=2)	Description
$K_{i,c}$	1.350	1.467	Convective hindrance factor
$K_{i,d}$	0.0337	0.2058	Diffusive hindrance factor
Φ_i	0.0924	0.2894	Steric coefficient

Table 4: Universal constants

Param.	Value	Description
F	96487	Faraday's constant ($C \cdot mol^{-1}$)
R_G	8.314	Gas perfect constant ($J \cdot mol \cdot K^{-1}$)

Table 5: Other variables

Param.	Description
J_i	solute flux ($mol \cdot m^{-2} \cdot s^{-1}$)
R	observed salt rejection (%)
λ_i	ratio of the Stokes radius of the solute i to the effective pore radius
μ	dynamic viscosity of solution ($kg \cdot m \cdot s^{-1}$)
Ψ_m	electric potential in the membrane (V)
∇V	Gradient potential ($V \cdot m^{-1}$)
ΔP	Pressure difference ($N \cdot m^{-2}$)